© 2017. Published by The Company of Biologists Ltd | Development (2017) 144, 1629-1634 doi:10.1242/dev.144436

RESEARCH REPORT

Hox-mediated endodermal identity patterns pharyngeal muscle formation in the chordate pharynx

Keita Yoshida[1,‡], Azusa Nakahata[1], Nicholas Treen[1,*], Tetsushi Sakuma[2], Takashi Yamamoto[2] and Yasunori Sasakura[1]

ABSTRACT

The chordate pharynx, possessing gill slits and the endostyle, is a complex of multiple tissues that are highly organized along the anterior-posterior (AP) axis. Although Hox genes show AP coordinated expression in the pharyngeal endoderm, tissue-specific roles of these factors for establishing the regional identities within this tissue have not been demonstrated. Here, we show that *Hox1* is essential for the establishment of AP axial identity of the endostyle, a major structure of the pharyngeal endoderm, in the ascidian *Ciona intestinalis*. We found that knockout of *Hox1* causes posterior-to-anterior transformation of the endostyle identity, and that *Hox1* represses *Otx* expression and anterior identity, and vice versa. Furthermore, alteration of the regional identity of the endostyle disrupts the formation of body wall muscles, suggesting that the endodermal axial identity is essential for coordinated pharyngeal development. Our results demonstrate an essential role of Hox genes in establishment of the AP regional identity in the pharyngeal endoderm and reveal crosstalk between endoderm and mesoderm during development of chordate pharynx.

KEY WORDS: Ascidian, *Ciona*, Endoderm, Hox, Pharyngeal muscle, Pharynx

INTRODUCTION

The pharynx, with gill slits and the endostyle (or thyroid gland), is a defining chordate feature, whereas the existence of gill slits can be extended to deuterostomes. The chordate pharynx comprises multiple tissues, such as nerves, muscles and endodermal epithelia, that are well organized along the embryonic anterior-posterior (AP) axis. Hox genes are thought to play important roles in establishing the regional identity of the pharynx along the AP axis (Couly et al., 1998; Gendron-Maguire et al., 1993; Hunt et al., 1991; Rijli et al., 1993). In the pharyngeal endoderm, Hox genes also exhibit coordinated expression during vertebrate development (Shone et al., 2016). In mice, loss of *Hoxa1* and *Hoxb1* functions results in absence of the third pharyngeal pouch derivatives, such as the thymus and parathyroid (Rossel and Capecchi, 1999). However, the tissue-specific role of Hox genes in the pharyngeal endoderm is not well understood, except for *Hoxa3*, which is involved in the development of the third pouch-derived organs (Chojnowski et al., 2014). A reason for the scarce understanding of the tissue-specific role of Hox genes is related to the multiplicity of their functions; Hox genes are expressed and function in various organs including pharyngeal endoderm. Therefore, little is known about how the regional identities are established within this tissue by Hox genes and how the patterning is coordinated with those in other tissues.

We have previously found that *Hox1* is expressed in the posterior part of the endostyle in the ascidian *Ciona intestinalis* (Sasakura et al., 2012). The endostyle is a mucus-producing organ formed on the ventral midline of the pharyngeal endoderm in non-vertebrate chordates and in larval lampreys, and is thought to be the precursor of the vertebrate thyroid gland (Salvatore, 1969). The ascidian endostyle is a representative structure of the pharynx and extends from the anterior to the posterior ends of the pharynx (Fig. 1K). Although *Hox1* expression in the posterior endostyle suggests involvement of this gene in AP patterning of the pharynx, its function is unclear. Here, we report an essential role of *Hox1* for establishing the AP axial identity of the endostyle in *Ciona*. We also find that the AP axial identity of the endostyle is necessary for the patterning of muscles in the pharynx, indicating that endodermal patterning is a key event for establishing the organized pharynx in chordates.

RESULTS AND DISCUSSION

Hox1 and *Otx* establish the regional identity of the endostyle

To explore the role of *Hox1* in the endoderm, we carried out tissue-specific knockout of *Hox1* using transcription activator-like effector nucleases (TALENs) (Treen et al., 2014). A TALEN pair designed to target the *Hox1* locus was expressed in the endodermal tissues under the control of *Titf1* regulatory sequence, which expresses downstream genes in the endoderm and a small subset of neural cells (Ristoratore et al., 1999; Sasakura et al., 2012). The endoderm-specific disruption of *Hox1* allowed embryos to develop to juveniles with normal atrial siphons and gill slits, both of which are lost in *Hox1* mutant animals (Sasakura et al., 2012). We first examined the expression of *Otx* and *Hox1*, which respectively mark the anterior and posterior endostyle as reported in another tunicate species (Cañestro et al., 2008) (Fig. 1A,E). Because TALENs generally introduce small deletions and/or insertions, expression of target genes usually remains in knockout animals, thereby allowing us to examine whether target genes are necessary for their own expression. Expression of *Hox1* in the posterior endostyle was not detected when *Hox1*-TALENs were expressed in the endodermal tissues (Fig. 1B). By contrast, *Otx* was ectopically expressed in the posterior endostyle in addition to the anterior endostyle (Fig. 1F). These results suggest that the identity of the posterior endostyle is transformed into the anterior one in the *Hox1* knockout juveniles, and that *Hox1* is required to repress the anterior identity in the posterior endostyle. Next, we tested whether *Hox1* is capable of

[1]Shimoda Marine Research Center, University of Tsukuba, 5-10-1 Shimoda, Shizuoka 415-0025, Japan. [2]Department of Mathematical and Life Sciences, Graduate School of Science, Hiroshima University, 1-3-1 Kagamiyama, Higashi-Hiroshima, Hiroshima 739-8526, Japan.
*Present address: Lewis-Sigler Institute for Integrative Genomics, Princeton University, NJ 08544, USA.

‡Author for correspondence (kyoshida@shimoda.tsukuba.ac.jp)

K.Y., 0000-0001-5557-9214

Received 5 September 2016; Accepted 7 March 2017

Development (2017) 144, 1629-1634 doi:10.1242/dev.144436

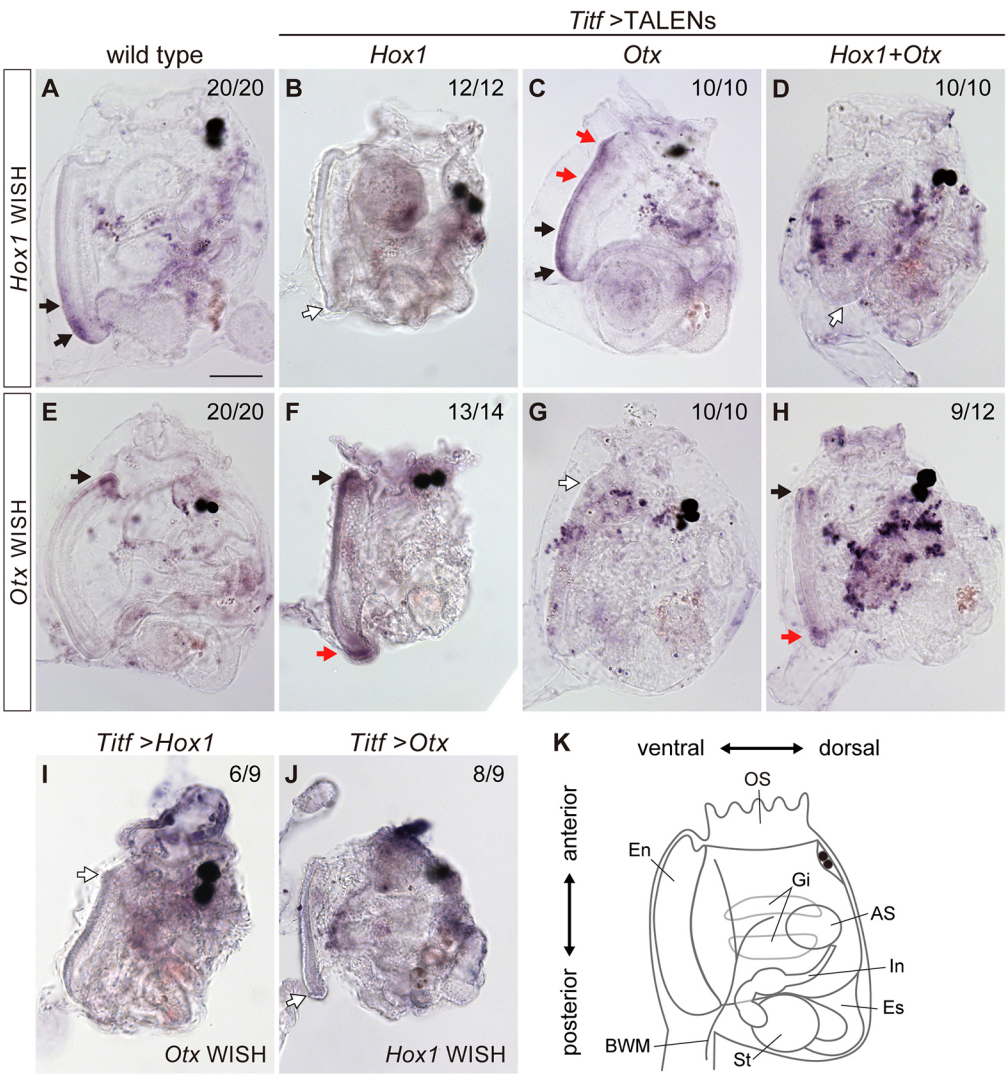

Fig. 1. *Hox1* and *Otx* establish the axial identity of the endostyle. (A-J) Whole-mount *in situ* hybridization (WISH) for *Hox1* (A-D,J) or *Otx* (E-I) in 6 dpf control (A,E), *Hox1*-TALEN-electroporated (B,F), *Otx*-TALEN-electroporated (C,G), *Hox1* and *Otx* double knockout (D,H), *Hox1*-overexpressing (I) and *Otx*-overexpressing (J) juveniles. Black, red and white arrows indicate normal, ectopic and loss of expression of analyzed gene, respectively. (K) A schematic of *Ciona* juvenile. AS, atrial siphon; BWM, body wall muscle; En, endostyle; Es, esophagus; Gi, gill; In, intestine; OS, oral siphon; St, stomach. In all panels, anterior is to the top and ventral is to the left. Numbers on the top right of panels indicate the proportion of juveniles showing the phenotype represented by the panel. Scale bar: 50 µm.

suppressing the anterior identity. Overexpression of *Hox1* in the endodermal tissues was carried out using the *Titf1 cis*-element (*Titf1>Hox1*). Expression of *Otx* was not detected in the anterior endostyle of *Titf1>Hox1*-electroporated animals (Fig. 1I), confirming that *Hox1* represses the anterior identity in the endostyle.

It has been reported that *Hox1* is expressed in the posterior trunk endoderm giving rise to the caudal pharynx at larval stages (Ikuta et al., 2004). To distinguish the role of *Hox1* in the endostyle from that in the larval endoderm, we expressed *Hox1*-TALENs using an enhancer that drives gene expression in the endostyle after metamorphosis (Awazu et al., 2004). The stage-limited knockout of *Hox1* recapitulated the ectopic expression of *Otx* in the posterior endostyle (Fig. S1). We also found that knockout of *Hox1* in the whole endoderm does not affect the expression of *Otx* at the larval stage (Fig. S1). These results indicate that the alteration of the posterior endostyle identity observed in *Hox1*-TALEN-electroporated juveniles is not a secondary effect of its disruption in the larval endoderm.

Next, we examined the role of *Otx* for establishing anterior identity in the endostyle. Knockout of *Otx* in the endoderm resulted in loss of *Otx* expression in the anterior endostyle (Fig. 1G). On the other hand, *Hox1* expression was expanded throughout the endostyle of juveniles electroporated with *Otx*-TALENs (Fig. 1C). These results indicate that *Otx* is required for establishing the anterior identity of the endostyle and repressing the posterior one. Then we carried out overexpression of *Otx* in the endoderm. Expression of *Hox1* in the posterior endostyle was not detected when *Titf1>Otx* was introduced (Fig. 1J). Taken together, these results suggest that *Hox1* and *Otx* play opposing roles in the organization of AP identity in the pharyngeal endoderm: *Hox1* establishes the posterior identity of the endostyle and represses *Otx* expression and subsequent anterior identity, and vice versa.

Because *Otx* is expressed in the endodermal cells of cleavage-stage embryos (Hudson and Lemaire, 2001), we examined whether the phenotypes seen in *Otx* knockout juveniles are the result of the disruption of this gene in early embryogenesis. First, we did not detect mutations in the *Otx* locus of early gastrula embryos electroporated with *Otx*-TALENs, but mutations were detectable at the larval stage (Fig. S1), suggesting that function of *Otx* in early development was not disrupted by TALENs expressed by the *Titf1* driver. We also found that expression of *Hox1* is not altered in the larvae electroporated with *Otx*-TALENs (Fig. S1). These results support the notion that expression of *Otx* in the anterior endostyle is required for establishing the anterior identity of the endostyle.

We also found that morphology of the endostyle depends on the molecular identity. The anterior tip of endostyle comprises large columnar cells and shows protruded morphology, whereas the

Development (2017) 144, 1629-1634 doi:10.1242/dev.144436

posterior tip has no such structure. In the *Hox1*-TALEN-electroporated juveniles, the posterior tip of the endostyle had the anterior-like morphology as well as expressing *Otx* (Fig. 1B,F; Fig. S1). On the other hand, the anterior tip became the posterior-like shape upon knockout of *Otx* (Fig. 1C,G; Fig. S1). These results indicate that morphology of the endostyle is determined by *Hox1* and *Otx*.

We next carried out simultaneous knockout of *Hox1* and *Otx* in the endoderm. In the double-knockout animals, *Hox1* expression was not detected whereas *Otx* was expressed in both the anterior and posterior endostyle (Fig. 1D,H). This result suggests that *Hox1* function is indispensable for *Hox1* expression itself, and the default identity of the posterior endostyle is the same as the anterior one expressing *Otx*.

A retinoic acid-*Hox1* feedback loop maintains the posterior identity

The default of anterior identity in the endostyle suggests that posterior identity with *Hox1* expression might require induction from other tissues. We investigated the mechanism that induces *Hox1* expression in the posterior endostyle. Retinoic acid (RA) is a well-known regulator of *Hox1* in *Ciona* (Kanda et al., 2009; Nagatomo and Fujiwara, 2003) as well as in vertebrates (Marshall et al., 1996). In *Ciona*, RA is involved in patterning of the central nervous system and posterior epidermis (Imai et al., 2009; Pasini et al., 2012). RA is also known to regulate endodermal patterning in tunicates (Hinman and Degnan, 1998, 2000). We carried out RA administration assay using the transgenic line EJ[MiTSAdTPOG]124 (hereafter referred to as EJ124), which is an enhancer trap line that expresses GFP under the control of a *Hox1* enhancer (Sasakura et al., 2012). GFP expression was detected throughout the endostyle of EJ124 juveniles cultured with RA after metamorphosis, suggesting that *Hox1* expression in the endostyle is activated by RA signaling (Fig. 2A,B). To determine whether RA signaling is necessary to induce *Hox1* expression in the posterior endostyle, we carried out endoderm-specific knockout of the retinoic acid receptor, *RAR* (Nagatomo et al., 2003). Expression of GFP in the posterior endostyle became detectable from 2 days post-fertilization (dpf) in control EJ124 animals (Fig. 2D). By contrast, GFP expression in the posterior endostyle was undetectable in EJ124 animals electroporated with TALENs for *RAR* (Fig. 2C). This suggests that *RAR* is indispensable for induction of *Hox1* expression in the posterior endostyle. We next analyzed expression of *Raldh2*, which encodes the RA-synthesizing enzyme (Zhao et al., 1996). *Raldh2* is expressed in a subset of tail muscle cells during embryogenesis (Nagatomo and Fujiwara, 2003). In addition, we found that *Raldh2* is expressed in the posterior trunk endoderm of swimming larvae (Fig. S2). To test whether RA synthesized in the larval tissues is required to induce *Hox1* expression in the endostyle, we carried out knockout of *Raldh2* in muscle and endodermal tissues simultaneously. Expression of *Hox1* in the posterior endostyle was diminished in animals electroporated with *Raldh2*-TALENs (Fig. S2), suggesting that RA signaling from larval muscle and endoderm induces *Hox1* expression in the endostyle.

To examine whether maintenance of the *Hox1* expression in the posterior endostyle depends on RA, we analyzed expression of *Raldh2* in juveniles. *Raldh2* was expressed in the posterior end of the endostyle in juveniles (Fig. 2I). This localized expression became evident after tail absorption (Fig. S2). Then we tested whether this localized *Raldh2* expression depends on the posterior identity of the endostyle. Expression of *Raldh2* was undetectable both in the *Hox1* knockout and in the *Otx*-overexpressing animals (Fig. 2J,K). On the other hand, overexpression of *Hox1* or knockout of *Otx* resulted in duplicated expression of *Raldh2* in both the anterior and posterior endostyle (Fig. 2L,M). These results suggest that expression of *Raldh2* in the posterior endostyle depends on *Hox1*-mediated posterior identity.

In order to test whether *Raldh2* in the endostyle is required for maintenance of *Hox1* expression, we carried out endoderm-specific knockout of *Raldh2* using EJ124 animals. GFP expression in the posterior endostyle was observed in *Raldh2*-TALEN-electroporated animals as well as in controls at 2 dpf (Fig. 2E,F), suggesting that *Raldh2* function in the endoderm is not necessary for initiation of *Hox1* expression in the endostyle. However, at 6 dpf, GFP expression in the posterior endostyle became hardly detectable in the *Raldh2* knockout animals (Fig. 2G,H). This indicates that RA synthesis in the posterior endostyle is required to maintain *Hox1* expression in the posterior endostyle. Taken together, these findings suggest that the RA-*Hox1* positive-feedback loop is necessary to establish the posterior identity of the endostyle: RA signaling from surrounding tail muscles and the posterior trunk endoderm can initiate *Hox1* expression in the posterior endostyle region; in turn *Hox1* upregulates *Raldh2* expression in the endostyle, and RA synthesized in the posterior endostyle maintains *Hox1* expression by the positive feedback (Fig. 2N). These data also suggest that the broader expression of *Hox1* throughout the endostyle observed in *Otx* knockout juveniles (Fig. 1C) is likely to be due to excess production of RA in both the anterior and posterior endostyle (Fig. 2M). We examined expression of *Raldh2* in larvae electroporated with TALENs targeting *Hox1*, *Otx* or *RAR*. Expression of *Raldh2* in the posterior trunk endoderm was unaffected by knockout of these genes (Fig. S2). This suggests that the RA-*Hox1* and *Otx* genetic network establishes the AP identity of pharyngeal endoderm during post-larval development.

Endodermal identity is essential for the directional elongation of body wall muscles

In order to address the significance of the regional identity of the endostyle for the development of the pharynx, we analyzed the formation of the body wall muscles (BWMs), which develop along the AP axis of the pharynx. Ascidian BWMs, as well as atrial siphon muscles, are specified through a shared genetic program with vertebrate pharyngeal muscles (Diogo et al., 2015; Stolfi et al., 2010). BWM precursor cells are located in the atrial siphon primordium before metamorphosis and BWMs elongate posteriorly towards the endostyle during metamorphosis (Stolfi et al., 2010) (Fig. 3A). Formation of BWMs was observed by expression of *Myosin heavy chain 3* (*Mhc3*) gene, which marks the oral and atrial siphon muscles and BWMs (Stolfi et al., 2010). We found that BWMs failed to elongate towards the posterior endostyle when *Hox1* was knocked out in the endoderm. In *Hox1* knockout juveniles, approximately 45% of observed BWMs displayed misdirected elongation (Fig. 3B) and 29% of them did not show elongation (Fig. 3C). These results suggest that the posterior identity of the endostyle is required for the directional elongation of BWMs towards the posterior endostyle. Because the endostyle and the atrial siphon, where precursors of BWMs are situated, are not adjacent to each other, there must be a signaling factor that is downstream of *Hox1* and promotes the directional elongation of BWMs. RA is a feasible candidate factor to promote the posterior elongation of BWMs. To test this possibility, we examined the BWM formation in the animals treated with an RA synthesis inhibitor, citral (Kanda et al., 2009; Marsh-Armstrong et al., 1994). In the citral-treated condition, BWMs seemed to start the posterior elongation process but failed to complete it (Fig. 3D,E). Then we observed BWM

Development (2017) 144, 1629-1634 doi:10.1242/dev.144436

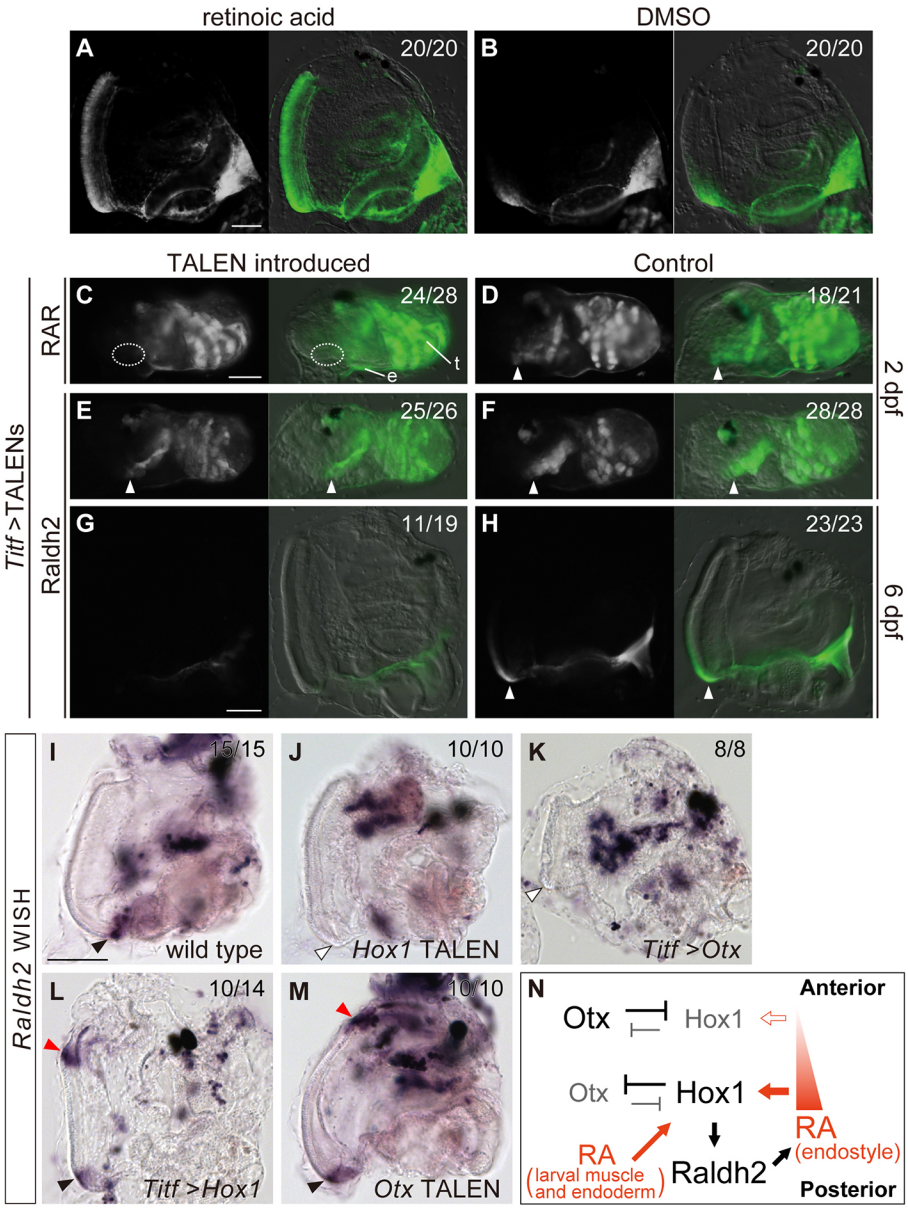

Fig. 2. Retinoic acid-*Hox1* feedback establishes the posterior identity. (A-H) Transgenic line of GFP enhancer trap for *Hox1*. In each panel, GFP fluorescence image (pseudocolored) is on the left and merged image of GFP and differential interference contrast is on the right. (A) An RA-treated 3 dpf juvenile. (B) A control juvenile. (C) An *RAR*-TALEN-electroporated 2 dpf juvenile. GFP expression was not observed in the posterior endostyle (dotted circle), but was observed in the epidermis (e) and autofluorescence of absorbed tail muscle (t) was detected. (D) A control juvenile. (E) A *Raldh2*-TALEN-electroporated 2 dpf animal. (F) A control 2 dpf animal. (G) A *Raldh2*-TALEN-electroporated 6 dpf juvenile. (H) A control 6 dpf juvenile. White arrowheads in D, E, F and H indicate GFP expression in the posterior endostyle. (I-M) Whole-mount *in situ* hybridization for *Raldh2* in 6 dpf juveniles. (I) A control juvenile. (J) A *Hox1*-TALEN-electroporated juvenile. (K) A *Otx*-overexpressing juvenile. (L) A *Hox1*-overexpressing juvenile. (M) A *Otx*-TALEN-electroporated juvenile. Black, red and white arrowheads indicate normal, ectopic and loss of *Raldh2* expression, respectively. (N) Model for the establishment of anterior-posterior identities in the endostyle. In all panels, anterior is to the top and ventral is to the left. Numbers on the top right of panels indicate the proportion of animals showing the phenotype represented by the panel. Scale bars: 50 µm.

formation in juveniles electroporated with *Raldh2* TALENs. Knockout of *Raldh2* in the endodermal tissue disrupted the elongation of BWMs (Fig. 3F,G), suggesting that RA synthesized in the posterior endostyle is required for posterior elongation of BWMs. Next, we treated juveniles with RA and analyzed BWM formation. In RA-treated animals, elongated BWMs were not observed, suggesting that ubiquitous RA input inhibits the elongation or differentiation of BWMs (Fig. S3). In order to clarify whether BWMs are not formed or failed to elongate by RA treatment, we carried out live imaging of BWM formation by expressing Kaede fluorescent protein in the BWMs with a *cis*-regulatory region of *Mhc3*. This imaging analysis revealed that BWMs made ectopic protrusions in various directions but the muscles failed to elongate in the posterior direction upon RA administration (Fig. 3H,I). These results further support the idea that RA synthesized in the posterior endostyle is necessary for directional elongation of the BWMs towards the posterior endostyle. It is also possible that there is another factor that regulates directional elongation of BWMs, because citral treatment or *Raldh2* knockout disrupted posterior elongation of BWMs but did not recapitulate the misdirected elongation observed in *Hox1* knockout animals. To understand fully the mechanism underlining the directional elongation of BWMs, identification of the factor(s) downstream of *Hox1* and/or *Otx* is necessary.

Conclusions

This study shows that in *C. intestinalis*, the anterior and posterior ends of the endostyle, a representative structure of pharyngeal endoderm, have distinct identities established by *Otx* and *Hox1* transcription factors, respectively. In chordates, these factors are expressed in the pharyngeal endoderm during embryogenesis. In mouse development, *Otx2* is expressed in the first arch endoderm (Ang et al., 1994), and *Hoxa1* and *Hoxb1* are expressed in the caudal pharynx in an RA- and *Raldh2*-dependent manner (Niederreither et al., 2003; Wendling et al., 2000). In the cephalochordate amphioxus, *Hox1* is expressed in the endoderm under the control of RA and represses *Otx* expression, which determines the posterior limit of the pharynx (Schubert et al., 2005). Therefore, the AP patterning mechanism of the *Ciona*

Development (2017) 144, 1629-1634 doi:10.1242/dev.144436

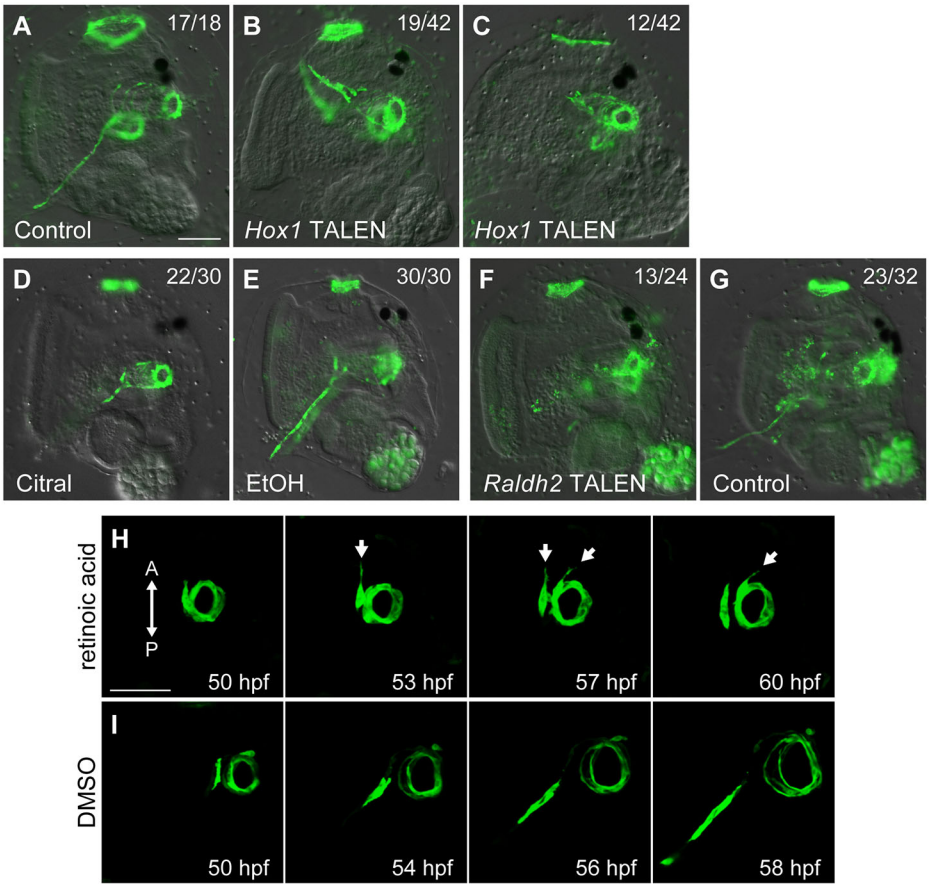

Fig. 3. Endodermal identity is essential for the directional elongation of BWMs. (A-G) Whole-mount *in situ* hybridization for *Mhc3* in 3 dpf juveniles. (A) A control juvenile. (B,C) *Hox1*-TALEN-electroporated juveniles. BWMs showed misdirected elongation (B) or no elongation (C). (D) A citral-treated juvenile. (E) A control animal treated with ethanol (EtOH). (F) A *Raldh2*-TALEN-electroporated juvenile. (G) A control juvenile. Numbers on the top right of panels indicate the proportion of BWMs showing the phenotype represented by the panel. (H,I) Time-lapse analysis of BWM formation using *Mhc3>Kaede*. 3D-reconstructed fluorescent images of the BWM and atrial siphon muscles are shown. Approximate developmental times are indicated on the bottom. Arrows indicate ectopic protrusions of BWMs. A, anterior; P, posterior. In all panels, anterior is to the top and ventral is to the left. Scale bars: 50 µm.

endostyle, involving *Otx* and RA-*Hox1*, might have utilized the shared genetic mechanism that patterns the AP axis of the early pharyngeal endoderm in chordate development.

In vertebrate pharyngeal development, patterning and differentiation of pharyngeal muscles are regulated by cranial neural crest cells (NCCs), which give rise to skeletal elements and tendons associated with muscles (Noden and Trainor, 2005; Rinon et al., 2007). Our present study demonstrates that proper formation of the BWM, a musculature surrounding the pharynx, is dependent on the regional identity of the endodermal organ. This suggests that in *Ciona*, which has no definitive NCC, it is primarily the endoderm that is responsible for organizing the pharynx along the AP axis.

MATERIALS AND METHODS

Animals

Wild-type *Ciona intestinalis* was cultivated at Maizuru (Kyoto), Misaki (Kanagawa), Mukaishima (Hiroshima) and Usa (Kochi). The transgenic line of the *Hox1* enhancer trap, EJ[MiTSAdTPOG]124, was maintained by an inland culture system (Joly et al., 2007).

Constructs and electroporation

TALENs were assembled using the four-module golden gate method (Sakuma et al., 2013). The activity of the constructed TALENs were estimated by previously described methods (Fig. S4) (Treen et al., 2014). Details of the construction of expression vectors and electroporation procedures are described in supplementary Materials and Methods.

Detection of mutations

Genomic DNAs were isolated from early gastrula embryos and swimming larvae developed from eggs, into which the *Titf1>Otx*-TALEN pair or the left side of *Otx*-TALEN (control) was electroporated, using the Wizard genomic DNA purification kit (Promega), and the genomic region including the target site of the *Otx*-TALEN pair was amplified by PCR. The PCR bands were analyzed by heteroduplex mobility shift assay with polyacrylamide gel electrophoresis (Ota et al., 2013) to examine their heterogeneity of the sequence that reflects the presence of the mutated gene.

RA and citral administration

Preparation of stock solutions of RA and citral was carried out as described previously (Kanda et al., 2009). Metamorphosing larvae were treated with 1 µM all-trans RA, 0.1% dimethylsulfoxide, 20 µM citral or 0.1% ethanol from 45 hours post-fertilization (hpf), which is prior to the onset of BWM elongation, to 62 hpf, after the posterior elongation of BWMs was complete.

In situ hybridization and imaging

Whole-mount *in situ* hybridization (WISH) was performed basically according to the previous study (Yoshida and Sasakura, 2012). Details of WISH and imaging are described in supplementary Materials and Methods.

Acknowledgements

We are grateful to the members of the Shimoda Marine Research Center at the University of Tsukuba for maintenance of transgenic animals and to Drs Shigeki Fujiwara, Kunifumi Tagawa, Nobuo Yamaguchi and all members of the Department of Zoology, Kyoto University, the Misaki Marine Biological Station, the University of Tokyo, and the Maizuru Fishery Research Station of Kyoto University for the cultivation and provision of wild-type *Ciona* adults. This study was further supported by the National BioResource Project, Japan.

Competing interests

The authors declare no competing or financial interests.

Author contributions

K.Y. and Y.S. designed the study. K.Y., A.N., N.T. and Y.S. performed the experiments. T.S. and T.Y. contributed materials for knockouts. K.Y., N.T. and Y.S. wrote the paper.

Development (2017) 144, 1629-1634 doi:10.1242/dev.144436

Funding
This work was supported by Grants-in-Aid for Scientific Research from the Japan Society for the Promotion of Science (20681019, 23681039, 16H04815).

Supplementary information
Supplementary information available online at
http://dev.biologists.org/lookup/doi/10.1242/dev.144436.supplemental

References

Ang, S. L., Conlon, R. A., Jin, O. and Rossant, J. (1994). Positive and negative signals from mesoderm regulate the expression of mouse Otx2 in ectoderm explants. *Development* **120**, 2979-2989.
Awazu, S., Sasaki, A., Matsuoka, T., Satoh, N. and Sasakura, Y. (2004). An enhancer trap in the ascidian Ciona intestinalis identifies enhancers of its Musashi orthologous gene. *Dev. Biol.* **275**, 459-472.
Cañestro, C., Bassham, S. and Postlethwait, J. H. (2008). Evolution of the thyroid: anterior-posterior regionalization of the Oikopleura endostyle revealed by Otx, Pax2/5/8, and Hox1 expression. *Dev. Dyn.* **237**, 1490-1499.
Chojnowski, J. L., Masuda, K., Trau, H. A., Thomas, K., Capecchi, M. and Manley, N. R. (2014). Multiple roles for HOXA3 in regulating thymus and parathyroid differentiation and morphogenesis in mouse. *Development* **141**, 3697-3708.
Couly, G., Grapin-Botton, A., Coltey, P., Ruhin, B. and Le Douarin, N. M. (1998). Determination of the identity of the derivatives of the cephalic neural crest: incompatibility between Hox gene expression and lower jaw development. *Development* **125**, 3445-3459.
Diogo, R., Kelly, R. G., Christiaen, L., Levine, M., Ziermann, J. M., Molnar, J. L., Noden, D. M. and Tzahor, E. (2015). A new heart for a new head in vertebrate cardiopharyngeal evolution. *Nature* **520**, 466-473.
Gendron-Maguire, M., Mallo, M., Zhang, M. and Gridley, T. (1993). Hoxa-2 mutant mice exhibit homeotic transformation of skeletal elements derived from cranial neural crest. *Cell* **75**, 1317-1331.
Hinman, V. F. and Degnan, B. M. (1998). Retinoic acid disrupts anterior ectodermal and endodermal development in ascidian larvae and postlarvae. *Dev. Genes Evol.* **208**, 336-345.
Hinman, V. F. and Degnan, B. M. (2000). Retinoic acid perturbs Otx gene expression in the ascidian pharynx. *Dev. Genes Evol.* **210**, 129-139.
Hudson, C. and Lemaire, P. (2001). Induction of anterior neural fates in the ascidian Ciona intestinalis. *Mech. Dev.* **100**, 189-203.
Hunt, P., Gulisano, M., Cook, M., Sham, M.-H., Faiella, A., Wilkinson, D., Boncinelli, E. and Krumlauf, R. (1991). A distinct Hox code for the branchial region of the vertebrate head. *Nature* **353**, 861-864.
Ikuta, T., Yoshida, N., Satoh, N. and Saiga, H. (2004). Ciona intestinalis Hox gene cluster: Its dispersed structure and residual colinear expression in development. *Proc. Natl. Acad. Sci. USA* **101**, 15118-15123.
Imai, K. S., Stolfi, A., Levine, M. and Satou, Y. (2009). Gene regulatory networks underlying the compartmentalization of the Ciona central nervous system. *Development* **136**, 285-293.
Joly, J.-S., Kano, S., Matsuoka, T., Auger, H., Hirayama, K., Satoh, N., Awazu, S., Legendre, L. and Sasakura, Y. (2007). Culture of Ciona intestinalis in closed systems. *Dev. Dyn.* **236**, 1832-1840.
Kanda, M., Wada, H. and Fujiwara, S. (2009). Epidermal expression of Hox1 is directly activated by retinoic acid in the Ciona intestinalis embryo. *Dev. Biol.* **335**, 454-463.
Marsh-Armstrong, N., McCaffery, P., Gilbert, W., Dowling, J. E. and Dräger, U. C. (1994). Retinoic acid is necessary for development of the ventral retina in zebrafish. *Proc. Natl. Acad. Sci. USA* **91**, 7286-7290.
Marshall, H., Morrison, A., Studer, M., Pöpperl, H. and Krumlauf, R. (1996). Retinoids and Hox genes. *FASEB J.* **10**, 969-978.
Nagatomo, K. and Fujiwara, S. (2003). Expression of Raldh2, Cyp26 and Hox-1 in normal and retinoic acid-treated Ciona intestinalis embryos. *Gene Expr. Patterns* **3**, 273-277.
Nagatomo, K., Ishibashi, T., Satou, Y., Satoh, N. and Fujiwara, S. (2003). Retinoic acid affects gene expression and morphogenesis without upregulating the retinoic acid receptor in the ascidian Ciona intestinalis. *Mech. Dev.* **120**, 363-372.
Niederreither, K., Vermot, J., Le Roux, I., Schuhbaur, B., Chambon, P. and Dollé, P. (2003). The regional pattern of retinoic acid synthesis by RALDH2 is essential for the development of posterior pharyngeal arches and the enteric nervous system. *Development* **130**, 2525-2534.
Noden, D. M. and Trainor, P. A. (2005). Relations and interactions between cranial mesoderm and neural crest populations. *J. Anat.* **207**, 575-601.
Ota, S., Hisano, Y., Muraki, M., Hoshijima, K., Dahlem, T. J., Grunwald, D. J., Okada, Y.' and Kawahara, A. (2013). Efficient identification of TALEN-mediated genome modifications using heteroduplex mobility assays. *Genes Cells* **18**, 450-458.
Pasini, A., Manenti, R., Rothbächer, U. and Lemaire, P. (2012). Antagonizing retinoic acid and FGF/MAPK pathways control posterior body patterning in the invertebrate chordate Ciona intestinalis. *PLoS ONE* **7**, e46193.
Rijli, F. M., Mark, M., Lakkaraju, S., Dierich, A., Dollé, P. and Chambon, P. (1993). A homeotic transformation is generated in the rostral branchial region of the head by disruption of Hoxa-2, which acts as a selector gene. *Cell* **75**, 1333-1349.
Rinon, A., Lazar, S., Marshall, H., Büchmann-Møller, S., Neufeld, A., Elhanany-Tamir, H., Taketo, M. M., Sommer, L., Krumlauf, R. and Tzahor, E. (2007). Cranial neural crest cells regulate head muscle patterning and differentiation during vertebrate embryogenesis. *Development* **134**, 3065-3075.
Ristoratore, F., Spagnuolo, A., Aniello, F., Branno, M., Fabbrini, F. and Di Lauro, R. (1999). Expression and functional analysis of Cititf1, an ascidian NK-2 class gene, suggest its role in endoderm development. *Development* **126**, 5149-5159.
Rossel, M. and Capecchi, M. R. (1999). Mice mutant for both Hoxa1 and Hoxb1 show extensive remodeling of the hindbrain and defects in craniofacial development. *Development* **126**, 5027-5040.
Sakuma, T., Ochiai, H., Kaneko, T., Mashimo, T., Tokumasu, D., Sakane, Y., Suzuki, K., Miyamoto, T., Sakamoto, N., Matsuura, S. et al. (2013). Repeating pattern of non-RVD variations in DNA-binding modules enhances TALEN activity. *Sci. Rep.* **3**, 3379.
Salvatore, G. (1969). Thyroid hormone biosynthesis in Agnatha and Protochordata. *Gen. Comp. Endocrinol. Supp.* **2**, 535-551.
Sasakura, Y., Kanda, M., Ikeda, T., Horie, T., Kawai, N., Ogura, Y., Yoshida, R., Hozumi, A., Satoh, N. and Fujiwara, S. (2012). Retinoic acid-driven Hox1 is required in the epidermis for forming the otic/atrial placodes during ascidian metamorphosis. *Development* **139**, 2156-2160.
Schubert, M., Yu, J. K., Holland, N. D., Escriva, H., Laudet, V. and Holland, L. Z. (2005). Retinoic acid signaling acts via Hox1 to establish the posterior limit of the pharynx in the chordate amphioxus. *Development* **132**, 61-73.
Shone, V., Oulion, S., Casane, D., Laurenti, P. and Graham, A. (2016). Mode of reduction in the number of pharyngeal segments within the sarcopterygians. *Zool. Lett.* **2**, 6.
Stolfi, A., Gainous, T. B., Young, J. J., Mori, A., Levine, M. and Christiaen, L. (2010). Early chordate origins of the vertebrate second heart field. *Science* **329**, 565-568.
Treen, N., Yoshida, K., Sakuma, T., Sasaki, H., Kawai, N., Yamamoto, T. and Sasakura, Y. (2014). Tissue-specific and ubiquitous gene knockouts by TALEN electroporation provide new approaches to investigating gene function in Ciona. *Development* **141**, 481-487.
Wendling, O., Dennefeld, C., Chambon, P. and Mark, M. (2000). Retinoid signaling is essential for patterning the endoderm of the third and fourth pharyngeal arches. *Development* **127**, 1553-1562.
Yoshida, R. and Sasakura, Y. (2012). Establishment of enhancer detection lines expressing GFP in the gut of the ascidian Ciona intestinalis. *Zoolog. Sci.* **29**, 11-20.
Zhao, D., McCaffery, P., Ivins, K. J., Neve, R. L., Hogan, P., Chin, W. W. and Dräger, U. C. (1996). Molecular identification of a major retinoic-acid-synthesizing enzyme, a retinaldehyde-specific dehydrogenase. *Eur. J. Biochem.* **240**, 15-22.

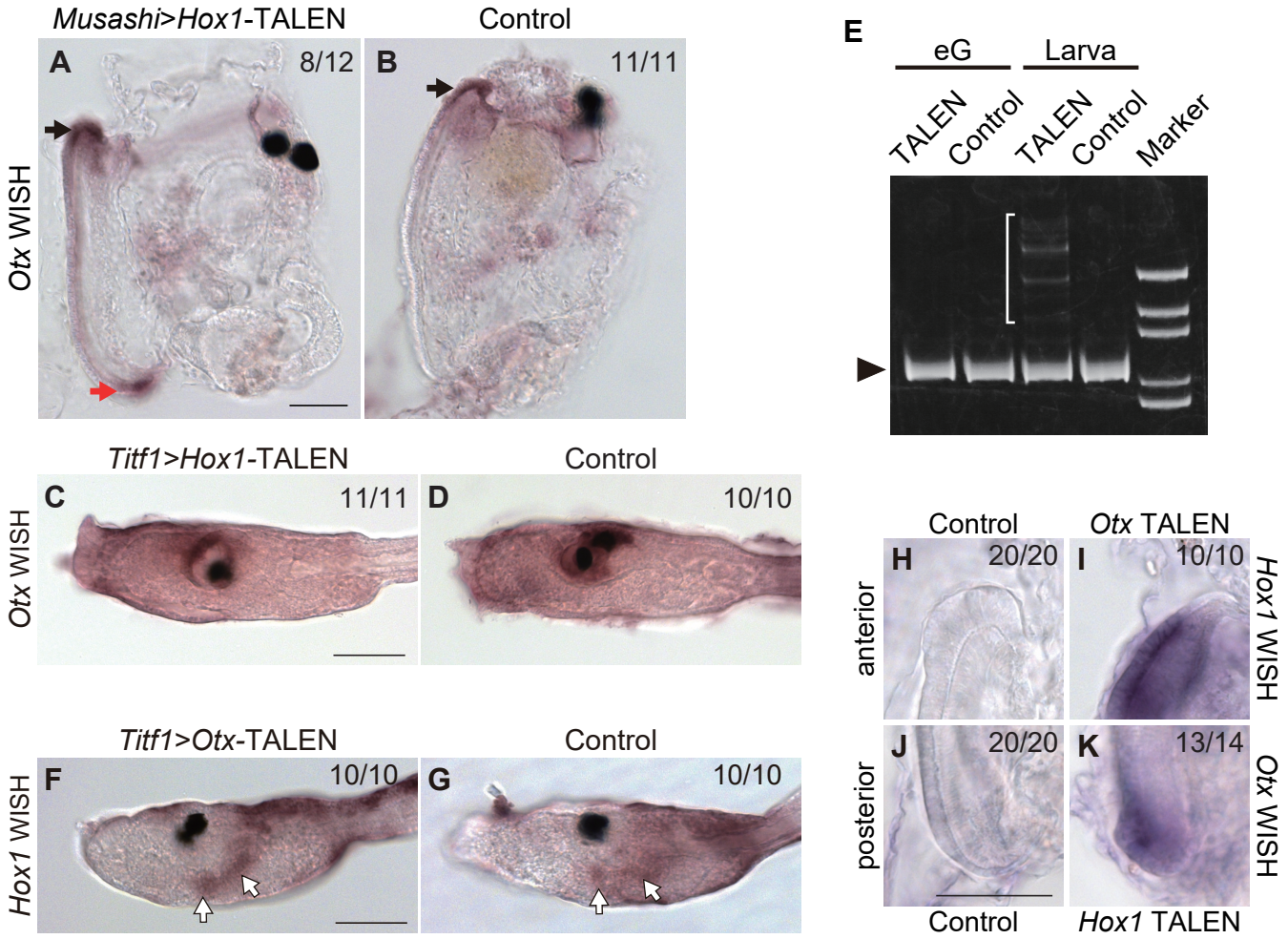

Figure S1. Functions of *Hox1* and *Otx* in the endostyle are required for establishing the identity of the posterior endostyle. (A, B) Whole-mount *in situ* hybridization (WISH) for *Otx* in 6 days post fertilization juveniles. (A) A *Musashi>Hox1*-TALEN introduced juvenile. (B) A control juvenile. One side of TALEN pair targeting *Hox1* was electroporated. When *Hox1* TALENs were expressed in the endostyle of juveniles, an ectopic expression of *Otx* in the posterior endostyle (red arrow) was detected in addition to the normal one in the anterior endostyle (black arrow). Anterior is to the top and ventral is to the left. (C, D) WISH for *Otx* in swimming larvae. (C) A *Titf1>Hox1*-TALEN introduced larva. (D) A control larva. Expression of *Otx* was detected only in the sensory vesicle in *Hox1*-TALEN introduced larvae as well as in control larvae. Anterior is to the left and dorsal is to the top. (E) Detection of mutations in the *Otx* locus of animals introduced with *Titf1>Otx*-TALENs. The PCR fragments containing the target site of *Otx*-TALEN were analyzed by heteroduplex mobility shift assay. The presence of shifted bands (brackets) indicates the formation of heteroduplexes with mismatched nucleotides, indicating the presence of mutations. The arrowhead indicates the position of PCR bands without mismatchs. Mutations in the *Otx* locus were only detectable in TALEN-introduced larvae. eG: early gastrula. (F, G) WISH for *Hox1* in swimming larvae. (F) A *Titf1>Otx*-TALEN introduced larva. (G) A control larva. Expression of *Hox1* in the endoderm marks presumptive posterior pharynx (white arrows). This expression pattern was not affected in *Otx*-TALEN introduced larvae. Anterior is to the left and dorsal is to the top. (H-K) Magnified images of the anterior (H, I) and posterior tips (J, K) of the endostyle in control (H, J), *Titf1>Hox1*- (K) and *Titf1>Otx*-TALEN (I) introduced animals. Numbers on the top right of panels indicate the proportion of larvae showing the phenotype represented by the panel. Scale bars: 50 μm.

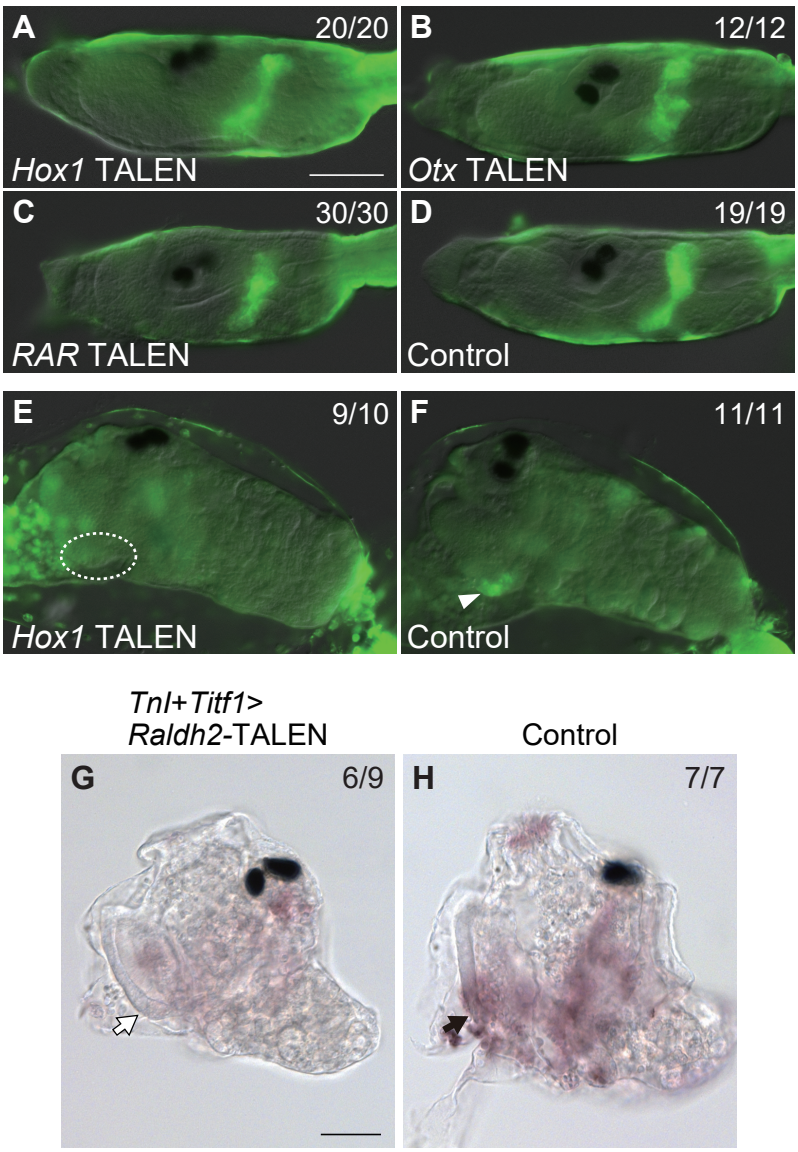

Figure S2. Retinoic acid synthesis in the larva is required for expression of *Hox1* in the posterior endostyle. (A-D) Whole-mount *in situ* hybridization (WISH) for *Raldh2* in swimming larvae. (A) A *Titf1>Hox1*-TALEN introduced larva. (B) A *Titf1>Otx*-TALEN introduced larva. (C) A *Titf1>RAR*-TALEN introduced larva. (D) A control larva. Expression of *Raldh2* was detected in the posterior trunk endoderm and anterior tail muscle cells. This expression pattern was not affected by knockout of *Hox1*, *Otx* or *RAR*. (E, F) WISH for *Raldh2* in tail-absorbed animals (30 hpf). (E) A *Titf1>Hox1*-TALEN introduced animal. Expression of *Raldh2* in the posterior endostyle was not observed (dotted circle). (F) A control animal. Expression of *Raldh2* was detected in the posterior endostyle (arrow head). Anterior is to the left and dorsal is to the top. (G, H) WISH for *Hox1* in 3 days post fertilization (dpf) juveniles. (G) A TALEN pair designed to target *Raldh2* were expressed in both muscle and endoderm. (H) A control juvenile. In *Raldh2*-TALEN introduced animal, expression of *Hox1* in the posterior endostyle was absent (white arrow), while this expression was detectable in the control animal (black arrow). Numbers on the top right of panels indicate the proportion of juveniles showing the phenotype represented by the panel. Scale bars: 50 μm.

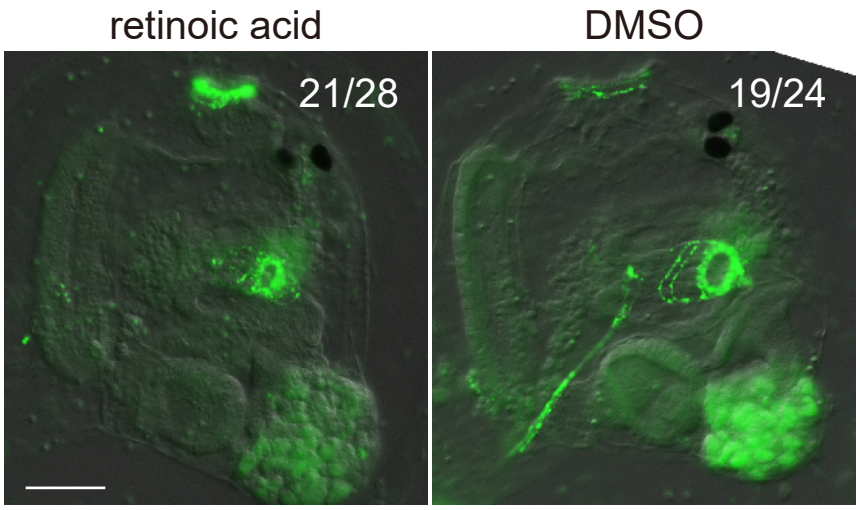

Figure S3. Retinoic acid disrupts posterior elongation of BWMs. Whole-mount in situ hybridization for *Mhc3* in 3 days post fertilization juveniles treated with retinoic acid or dimethylsulfoxide (DMSO). Numbers on the top right of panels indicate the proportion of BWMs showing the phenotype represented by the panel. Scale bar: 50 μm.

Hox1 TALEN

```
TTCACTACAAAACAGCTTACCGAGCTTGAAAAAGAGTTTCACTTCAATA

TTCACTACAAAACAGCT----------AAAAAGAGTTTCACTTCAATA  1x
TTCACTACAAAACAGCTT---------GAAAAAGAGTTTCACTTCAATA  1x
TTCAGTACAAAACAGCTTACCG----AAAAAAAGAGTTTCACTTCAATA  1x
TTCACTACAAAACAGCTTACCGA------AAAAGAGTTTCACTTCAATA  1x
TTCACTACAAAACAGCTTACCGAATTTCACTACAAAACAGCTTACCTTG
AAAAAGAGTTTCACTTCAATA                              1x
```

Mutation frequency 100% (n=5)

Otx TALEN

```
TCGGAAAGACAAGATATCCCGATATCTTTATGAGAGAAGAAGTTGCCCTA

TCGGAAAGACAAGATATCCCGA----------GAGAAGAAGTTGCCCTA  1x
TCGGAAAGACAAGATAT-------ATATTATGAGAGAAGAAGTTGCCCTA  1x
TCGGAAAGACAAGAT-----------TATGAGAGAAGAAGTTGCCCTA  1x
TCGGAAAGACAAGATAT----------TTATGAGAGAAGAAGTTGCCCTA  1x
TCGGAAAGACAAGATAT----------TATGAGAGAAGAAGTTGCCCTA  1x
TCGGAAAGACAAGATATCCCGATATCTTTATGAGAGAAGAAGTTGCCCTA  1x
```

Mutation frequency 83.3% (n=6)

RAR TALEN

```
TTCTTTCGACGTAGTGTGCAGAAGAACATGCAGTATACTTGTCATCGTAACA

TTCTTTCGACGTAGTGTGCAGAA-----TGCAGTATACTTGTCATCGTAACA  1x
TTCTTTCGACGTAGTGTGCAGAA------GCAGTATACTTGTCATCGTAACA  1x
TTCTTTCGACGTAGTGTGCAGAA---------GTATACTTGTCATCGTAACA  1x
TTCTTTCGACGTAGTGTGCAGA----------ATACTTGTCATCGTAACA  2x
TTCTTTCGACGTAGTGTGCAG----------TATACTTGTCATCGTAACA  2x
TTCTTTCGACGTAGTGTGCAGAAGAACATGCAGTATACTTGTCATCGTAACA  1x
```

Mutation frequency 87.5% (n=8)

Raldh2 TALEN

```
TTCAGTCGTATCAGCAGTACCAGCAGCCTCTCAAATCCCCGAGGTGAACA

TTCAGTCGTATCAGCAGTACC------CTCTCAAATCCCCGAAGTGAACA  2x
TTCAGTCGTATCAGCAGTACC-------TCTCAAATCCCCGAAGTGAACA  2x
TTCAGTCGTATCAGCAGTACCAGC----TCTCAAATCCCCGAAGTGAGCA  4x
TTCAGTCGTATCAGCAGTACC---CCCCTCTCAAATCCCCGAAGTGAACA  1x
TTCAGTCGTATCAGCAGTACCAGTCAAATAAACATAAGCTTTATCAGCAG
TACCCGTATCAGCAGTACCAGTCCTCTCAAATCCCCGAAGTGAACA      1x
```

Mutation frequency 100% (n=10)

Figure S4. Activity of TALENs. Examples of the sequenced mutations found in animals introduced with a TALEN pair targeting *Hox1*, *Otx*, *RAR* or *Raldh2*. PCR fragments that include the binding sites of each TALEN pair were sequenced. Sequence of wild type genome is shown on the top. TALEN binding regions are highlighted in blue. "-" represents deletion of a nucleotide. The nucleotides that were not seen in the normal sequence are shown in red. The number at the right side indicate the frequency of the appearance.

Supplementary Materials and Methods

Constructs

TALENs were assembled by 4-module golden gate method (Sakuma et al., 2013). The previously described TALEN structure (Treen et al., 2014) was simplified by putting the TALEN and mCherry on a single ORF separated by a 2A peptide sequence (GSGEGRGSLLTCGDVEENPGP) (Szymczak et al., 2004) by amplifying the backbone TALEN and 2A::mCherry insert by PCR with 15bp overlapping regions and recombining them using an In-Fusion HD cloning kit (Clontech). The activity of the constructed TALENs were estimated by expressing under the control of the *EF1α* promoter according to the previous method (Treen et al., 2014) (Figure S6). The *EF1α* promoter was replaced with the promoter of *Titf1* (Sasakura et al., 2012) for endoderm-specific expressions using the In-Fusion HD cloning kit. An enhancer element of *Musashi* gene (designated as fragment 3) fused with the *TPO* promoter (Awazu et al., 2004) was used to drive TALEN expression in the endostyle of juveniles. For driving TALEN expression in the muscle lineage, the *EF1α* promoter was replaced with the promoter of *TnI* (Davidson and Levine, 2003). The *Titf1>Hox1* construct was described previously (Sasakura et al., 2012). The promoter of *Titf1* and cDNA of *Otx* (Ciinte.CG.KH2012.C4.84) was amplified by polymerase chain reaction (PCR) using following primer pairs (F: 5'- CGACTCTAGAGGATCCTAGTTCATGGTTAGCAATGAC-3'; R: 5'-GGCCGCAAGGGGATCCTCACAGCAAAGTTTCCAGTG-3') and (F: 5'-GATCCCCTTGCGGCCATGTCGTATTTGAAATCTCCC-3'; R: 5'-CCTGATCCTGCGGCCGCCAAGACTTGGAATTTCC-3'), respectively. PCR fragments of *Titf1* promoter and *Otx* cDNA are fused with 2A::mCherry using the In-Fusion HD cloning kit to create *Titf1>Otx*. Genomic upstream region of *Mhc3* (Ciinte.CG.KH2012.C3.774) was isolated by PCR from *Ciona* genomic DNA using following primers (F: 5'-AATCTGCAGTAAAACGTCCGTTTCCGAAC-3'; R: 5'-TTTTCTAGATTTTCCCCACTTGAATCCAC-3') and inserted into the *Pst* I (5') and *Xba* I (3') sites of pSP-Kaede (Hozumi et al., 2010) to generate the *Mhc3>Kaede* construct. The official names of the vectors and transgenic lines according to the nomenclature rule of tunicates (Stolfi et al., 2015) were as follows: *Titf1>TALENs*, p*Ciinte*.REG.KH2012.C10.3638397-3636215|*Titf1>TALEN*::*2A*::*mCherry*; *Musashi>TALENs*, p*Ciinte*.REG.KH2012.C10.4438567-4440059|*Musashi*:*Ciinte*.REG.KH2012.L3.178445-177583|*Tpo> TALEN*::*2A*::*mCherry*; *TnI>TALENs*, p*Ciinte*.REG.KH2012.C11.1684372-1685258|*TnI>TALEN*::*2A*::*mCherry*;

Titf1>Hox1, p*Ciinte*.REG.KH2012.C10.3638397-3636215|*Titf1>CFP*::*Hox1*; *Titfi>Otx*, p*Ciinte*.REG.KH2012.C10.3638397-3636215|*Titf1>Otx*::*2A*::*mCherry*; *Mhc3>Kaede*, p*Ciinte*.REG.JGIv2.chr03q.1986302-1989326|*Mhc3>Kaede*; EJ[MiTSAdTPOG]124, *Ciinte*.E[pMi-TSA-*Ciinte*.REG.KH2012.L3.178445-177583|*Tpo>GFP*]124.KH2012.L171.188604.

Electroporation

Plasmid DNAs were electroporated to 1-cell embryos according to the previous reports (Corbo et al., 1997; Treen et al., 2014). Dechorionated eggs of wild type animals were inseminated with sperm isolated from wild type or EJ[MiTSAdTPOG]124 (EJ124) (Sasakura et al., 2012) animals. In knockout experiments, 20 μg (*Hox1*- and *Otx*-TALENs) or 30 μg (*RAR*- and *Raldh2*-TALENs) of expression vectors of L and R TALENs were electroporated for each electroporation. For control of knockout experiments, twofold amount of expression vectors of only one side of each TALEN pair (L or R) were electroporated. In the other experiments, 30 μg of DNA was electroporated. Animals with strong RFP (in *Titf1>TALEN*s or *Titf1>Otx* electroporation) or CFP (in *Titf1>Hox1* electroporation) fluorescence in the endoderm were selected at the tailbud stage for further culturing. Individuals expressing GFP were selected among animals developed from eggs inseminated with EJ124 sperm at 2 days post fertilization for further experiment.

***In situ* hybridization and imaging**

Whole-mount *in situ* hybridization (WISH) was done basically according to the previous study (Ikuta et al., 2010; Yoshida and Sasakura, 2012) with some modifications described below: juveniles of appropriate stages were relaxed with L-menthol and fixed with 4% formaldehyde in seawater for at least three days at 4°C; and after incubation with proteinase K, specimens were washed four times with PBST and then tunics were removed manually using tungsten needles. The signals were visualized with nitro-blue tetrazolium chloride and 5-bromo-4-chloro-3′-indolyphosphate substrates or with TSA Plus Fluorescein Kit (Perkin Elmer). Digoxigenin-labeled RNA probes for *Otx* (Ciinte.CG.KH2012.C4.84), *Raldh2* (Ciinte.CG.KH2012.C4.697) and *Mhc3* (Ciinte.CG.KH2012.C3.774) were synthesized using Gateway ORF clones (Roure et al., 2007) as templates. RNA probes for *Hox1* (Ciinte.CG.KH2012.L171.16) was described previously (Sasakura et al., 2012). The WISH images are acquired by Axio Observer.Z1 and AxioCam MRm (Carl Zeiss).

Fluorescent images were taken with a Zeiss fluorescent microscope AxioImager.Z1 and AxioCam MRm. For time-lapse imaging of BWM formation, embryos were electroporated with *Mhc3*>Kaede at the 1-cell stage. At 48-50 hours post fertilization, individuals were mounted on a glass-based dish (Iwaki) and time-lapse 3D imaging was performed using LSM700 confocal microscope (Carl Zeiss). The recording interval was 10 min. Three-dimensional images were reconstructed from z-stack images using ZEN2010 software (Carl Zeiss).

Supplementary Reference

Awazu, S., Sasaki, A., Matsuoka, T., Satoh, N. and Sasakura, Y. (2004). An enhancer trap in the ascidian Ciona intestinalis identifies enhancers of its Musashi orthologous gene. *Dev Biol* **275**, 459-472.

Corbo, J. C., Levine, M. and Zeller, R. W. (1997). Characterization of a notochord-specific enhancer from the Brachyury promoter region of the ascidian, Ciona intestinalis. *Development* **124**, 589-602.

Davidson, B. and Levine, M. (2003). Evolutionary origins of the vertebrate heart: Specification of the cardiac lineage in Ciona intestinalis. *Proc Natl Acad Sci U S A* **100**, 11469-11473.

Hozumi, A., Kawai, N., Yoshida, R., Ogura, Y., Ohta, N., Satake, H., Satoh, N. and Sasakura, Y. (2010). Efficient transposition of a single Minos transposon copy in the genome of the ascidian Ciona intestinalis with a transgenic line expressing transposase in eggs. *Dev Dyn* **239**, 1076-1088.

Ikuta, T., Satoh, N. and Saiga, H. (2010). Limited functions of Hox genes in the larval development of the ascidian Ciona intestinalis. *Development* **137**, 1505-1513.

Roure, A., Rothbächer, U., Robin, F., Kalmar, E., Ferone, G., Lamy, C., Missero, C., Mueller, F. and Lemaire, P. (2007). A multicassette Gateway vector set for high throughput and comparative analyses in ciona and vertebrate embryos. *PLoS One* **2**, e916.

Sakuma, T., Ochiai, H., Kaneko, T., Mashimo, T., Tokumasu, D., Sakane, Y., Suzuki, K., Miyamoto, T., Sakamoto, N., Matsuura, S., et al. (2013). Repeating pattern of non-RVD variations in DNA-binding modules enhances TALEN activity. *Sci Rep* **3**, 3379.

Sasakura, Y., Kanda, M., Ikeda, T., Horie, T., Kawai, N., Ogura, Y., Yoshida, R., Hozumi, A., Satoh, N. and Fujiwara, S. (2012). Retinoic acid-driven Hox1 is required in the epidermis for forming the otic/atrial placodes during ascidian metamorphosis. *Development* **139**, 2156-2160.

Stolfi, A., Sasakura, Y., Chalopin, D., Satou, Y., Christiaen, L., Dantec, C., Endo, T., Naville, M., Nishida, H., Swalla, B. J., et al. (2015). Guidelines for the nomenclature of genetic elements in tunicate genomes. *Genesis* **53**, 1-14.

Szymczak, A. L., Workman, C. J., Wang, Y., Vignali, K. M., Dilioglou, S., Vanin, E. F. and Vignali, D. A. (2004). Correction of multi-gene deficiency in vivo using a single 'self-cleaving' 2A peptide-based retroviral vector. *Nat Biotechnol* **22**, 589-594.

Treen, N., Yoshida, K., Sakuma, T., Sasaki, H., Kawai, N., Yamamoto, T. and Sasakura, Y. (2014). Tissue-specific and ubiquitous gene knockouts by TALEN electroporation provide new approaches to investigating gene function in Ciona. *Development* **141**, 481-487.

Yoshida, R. and Sasakura, Y. (2012). Establishment of enhancer detection lines expressing GFP in the gut of the ascidian Ciona intestinalis. *Zoolog Sci* **29**, 11-20.